

# Effect of spin-lattice relaxation on the Mössbauer spectrum of metmyoglobin

A. M. Afanas'ev, E. Yu. Tsymbal, V. M. Cherepanov, N. A. Chuev, S. S. Yakimov, and F. Parak<sup>1)</sup>

*I. V. Kurchatov Institute of Atomic Energy*

(Submitted 30 October 1986)

*Zh. Eksp. Teor. Fiz.* **92**, 2209–2219 (June 1987)

The Mössbauer spectrum of a metmyoglobin single crystal in a “stabilizing” magnetic field  $H_e \approx 200$  G is investigated for temperatures in the 4.2–57 K range. The influence of spin-lattice relaxation on the hyperfine structure of the Mössbauer spectrum of the  $^{57}\text{Fe}^{3+}$  ion in an axial crystal field is analyzed for the first time in a complete manner. A four-level model for the electron shell of the  $\text{Fe}^{3+}$  ion is used to find the temperature dependence of the relaxation parameters  $\gamma_1$  and  $\gamma_2$ . The dependence points to a single-phonon relaxation mechanism and indicates that the vibrations of the paramagnetic complex are strongly anisotropic.

## 1. INTRODUCTION

The Mössbauer spectra for paramagnetic ions in diamagnetic crystal lattices show a well-resolved hyperfine structure at low concentrations and temperatures, because the electron spin relaxes quite slowly. As the temperature increases the lattice vibrations modulate the frequencies of the nuclear transitions, and the resulting spectral broadening depends both on the nature of the spin-lattice relaxation and on the phonon spectrum of the crystal. The form of the relaxation Mössbauer spectrum and its temperature dependence can be used in principle to deduce the relaxation mechanism and to determine the vibrational structure of the paramagnetic ion/ligand complex.

In spite of the great diversity of the theoretical methods, however, almost all of the available experimental data on the effects of electron relaxation on Mössbauer hyperfine structure have so far been interpreted using a single very simple model in which a single parameter, the effective relaxation rate  $\gamma$ , describes the transitions among the sublevels of the fine structure (see, e.g., Ref. 1). It is clear that such a model can yield only qualitative information about the relaxation process, since in general the relaxation must be described by several constants  $\gamma_i$  whose number depends on symmetry considerations.<sup>2,3</sup>

One reason for this state of affairs is the difficulty in mathematically analyzing the relaxation spectra; matrices of large rank must be inverted in order to solve the secular equation. Another difficulty stems from the way the paramagnetic hyperfine structure is formed in real crystals. The electron Zeeman energy  $\mathcal{H}_Z$  in a magnetic field may be comparable to the hyperfine interaction energy  $\mathcal{H}_{HF}$ , so that a mixed electron-nuclear system of levels is produced. In addition to the state of the nucleus, the state of the electron shell may then also change during the Mössbauer transitions, with some of the energy of the nuclear transition being provided by the electron Zeeman energy. For the case of the  $^{57}\text{Fe}^{3+}$  ion, e.g., the hyperfine spectra are therefore extremely sensitive to the weak random magnetic fields  $H_r \sim 10$  G generated by the magnetic moments of nearby nuclei and paramagnetic ions.<sup>3</sup> If in addition the hyperfine interaction is only slightly anisotropic, these fields will greatly broaden the Mössbauer spectrum even when the relaxation process occurs slowly. To restore a well-resolved hyperfine structure, one must ensure that  $\mathcal{H}_Z$  is much larger

than  $\mathcal{H}_{HF}$  by adding a stabilizing external field  $H_e \sim 10^2$  G; the Mössbauer transitions will then be purely nuclear.<sup>4</sup>

These are several reasons why myoglobin macromolecules<sup>5</sup> are particularly well suited for detecting a dependence of the spin-lattice relaxation process on more than one parameter. First, spin-spin interactions have little influence on the relaxation owing to the large distance (30 Å) between adjacent  $\text{Fe}^{3+}$  ions in myoglobin crystals. Second, the crystal field produced by the nearest neighbors at an  $\text{Fe}^{3+}$  ion is so strong that the Stark splitting of the ground state approaches the maximum splitting yet reported for the high-spin  $\text{Fe}^{3+}$  ion; therefore, only the doublet  $|\pm 1/2\rangle$  is appreciably populated at liquid helium temperatures, which makes the Mössbauer spectra much easier to analyze. Finally, the theoretical analysis in Ref. 6 shows that because the crystal field in myoglobin is axisymmetric, only two parameters  $\gamma_1$  and  $\gamma_2$  are needed to describe the diverse effects of relaxation on the Mössbauer spectra.

In this paper we investigate how the electron spin-lattice relaxation and the random magnetic field affect the paramagnetic hyperfine structure in Mössbauer spectra for  $^{57}\text{Fe}^{3+}$  ions in a metmyoglobin single crystal Mb( $\text{H}_2\text{O}$ ).

## 2. THEORY

The monoclinic unit cell of myoglobin (space group  $P2_1c$ , lattice parameters<sup>7</sup>  $a = 64.6$  Å,  $b = 31.1$  Å,  $c = 34.8$  Å,  $\beta = 105.5^\circ$ ) contains two molecules which are interchanged by a  $180^\circ$  rotation about the unique symmetry axis  $[b]$ . Each molecule contains a heme complex with an octahedrally coordinated  $\text{Fe}^{3+}$  ion. The angle between the  $z$ -axes of the complexes (between the normals  $\mathbf{n}_1$  and  $\mathbf{n}_2$  to the hemes, Fig. 1) is  $\theta = 44^\circ$ . The two positions of the  $\text{Fe}^{3+}$  ion are thus magnetically inequivalent, and each gives rise to a partial spectrum.

To first order the crystal field has the tetragonal symmetry  $C_{4v}$ , and its Hamiltonian is expressible in the axisymmetric form

$$\mathcal{H}_{CF} = D[S_z^2 - 1/3 S(S+1)]. \quad (1)$$

Here we have omitted the small rhombic distortion parameter<sup>8</sup>;  $S$  is the nuclear spin, and  $D$  is the crystal field parameter. The Hamiltonian  $\mathcal{H}_{CF}$  splits the ground term  $^6S_{5/2}$  of the  $\text{Fe}^{3+}$  ion into three Kramers doublets (Fig. 2a). Only the  $|\pm 1/2\rangle$  doublet is appreciably populated at helium tem-

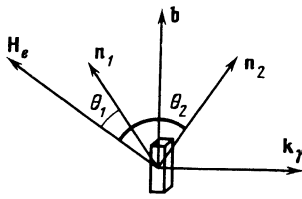


FIG. 1. Experimental geometry. The external magnetic field  $\mathbf{H}_e$  makes the angles  $\theta_1, \theta_2$  with the heme normals  $\mathbf{n}_1, \mathbf{n}_2$ , which coincide with the  $z_1$  and  $z_2$  axes of the axisymmetric magnetically inequivalent  $\text{Fe}^{3+}$  ion complexes. The angle between  $\mathbf{n}_1$  and  $\mathbf{n}_2$  is  $\theta = 44^\circ$ ;  $[b]$  is the two-fold symmetry axis;  $\mathbf{k}_\gamma$  is the direction of the gamma-photon beam.

peratures; all the components of its  $g$ -tensor are nonzero, which explains its sensitivity to the magnitude and direction of the magnetic field. Since the doublets  $|\pm 3/2\rangle$  and  $|\pm 5/2\rangle$  are separated by  $\Delta = 2D \approx 20$  K and  $3\Delta \approx 60$  K, respectively, from the lowest doublet, the hyperfine structure can be analyzed for the temperature range of interest by using a four-level electron system consisting of the doublet  $|\pm 1/2\rangle$  in the ground state and the doublet  $|\pm 3/2\rangle$  in the excited state.

The two doublets can be regarded as independent for weak magnetic fields, and they are characterized by their Zeeman and hyperfine interactions. The structure of their electron-nuclear levels can be described in terms of the effective spin  $S' = 1/2$  by using the Hamiltonian<sup>9</sup>

$$\mathcal{H}^{(i)} = \mathcal{H}_z^{(i)} + \mathcal{H}_{HF}^{(i)} + \mathcal{H}_Q = \mu_B \mathbf{H} \hat{g}^{(i)} \mathbf{S}' + \mathbf{I} \hat{A} \mathbf{S}' + eQV_{zz} [3I_z^2 - I(I+1)] / 4I(2I-1). \quad (2)$$

Here  $\mathcal{H}_Q$  is the Hamiltonian for the quadrupole interaction,  $\hat{A}$  is the hyperfine interaction tensor,  $V_{zz}$  is the electric field gradient tensor at the nucleus,  $Q$  is the nuclear quadrupole moment,  $I$  is the nuclear spin,  $\mathbf{H} = \mathbf{H}_e + \mathbf{H}_r$ , and the superscript  $i = 1, 2$  labels the doublets, which have the following parameters ( $A$  is the hyperfine interaction constant):

$i$	$S$	$g_{xx}$	$g_{yy}$	$g_{zz}$	$A_{xx}$	$A_{yy}$	$A_{zz}$
1	$\pm 1/2$	$\frac{6}{6}$	$\frac{6}{6}$	$\frac{2}{6}$	$3A$	$3A$	$A$
2	$\pm 3/2$	0	0	6	0	0	$3A$

In an external magnetic field  $H_e \sim 10^2$  G we have  $\mathcal{H}_z \gg \mathcal{H}_{HF}, \mathcal{H}_Q$ , and in this case the magnetic hyperfine

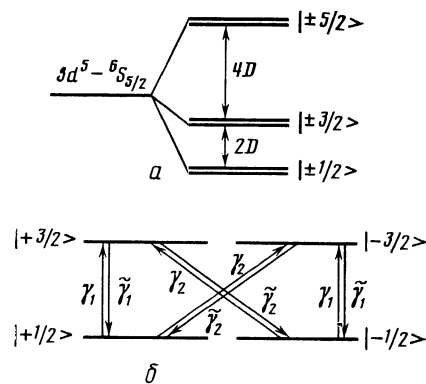


FIG. 2. a) Splitting of the ground-state term  $6S_{5/2}$  of the  $\text{Fe}^{3+}$  ion into three Kramer's doublets in an axisymmetric crystal field; b) relaxation transitions between the doublets  $|\pm 1/2\rangle$  and  $|\pm 3/2\rangle$ , assuming a four-level model for the  $\text{Fe}^{3+}$  electron shell.

interaction is describable in terms of the effective hyperfine field<sup>10</sup>:

$$\mathcal{H}_{HF}^{(i)} = \mu_n g_n \mathbf{H}_{eff}^{(i)} \mathbf{I}. \quad (4)$$

In the axisymmetric case,  $\mathbf{H}_{eff}^{(i)}$  depends only on the angle between the magnetic field  $\mathbf{H}$  and the  $z$  axis of the complex and is determined by its two projections

$$H_{eff\parallel}^{(i)} = \pm \frac{1}{2\mu_n g_n} \frac{A_{\parallel}^2 \cos \theta}{(A_{\parallel}^2 \cos^2 \theta + A_{\perp}^2 \sin^2 \theta)^{1/2}},$$

$$H_{eff\perp}^{(i)} = \pm \frac{1}{2\mu_n g_n} \frac{A_{\perp}^2 \sin \theta}{(A_{\parallel}^2 \cos^2 \theta + A_{\perp}^2 \sin^2 \theta)^{1/2}}, \quad (5)$$

where  $A_{\perp} = A_{xx}^{(i)} = A_{yy}^{(i)}, A_{\parallel} = A_{zz}^{(i)}$ .

We see from (3) and (5) that the doublet  $|\pm 3/2\rangle$  is insensitive to the magnitude and direction of the magnetic field, i.e., its wave functions do not change so long as  $\mathcal{H}_z \ll \mathcal{H}_{CF}$ :

$$|2^{(\pm)}\rangle = |\pm 3/2\rangle, \quad (6)$$

whereas an applied magnetic field transforms the wave functions for the doublet  $|\pm 1/2\rangle$  into

$$|1^{(+)}\rangle = a_1 |1/2\rangle + a_2 |-1/2\rangle, \quad (7)$$

$$|1^{(-)}\rangle = -a_2 |1/2\rangle + a_1 |-1/2\rangle,$$

where

$$a_{1,2} = [(w \pm \cos \theta) / 2w]^{1/2}, \quad w^2 = \cos^2 \theta + 9 \sin^2 \theta. \quad (8)$$

The lattice vibrations produce fluctuations in the crystal field acting on the paramagnetic ion  $\text{Fe}^{3+}$  and give rise to a spin relaxation of its electron shell. The general theory<sup>11</sup> gives the following expression for the Mössbauer absorption spectrum in a system with relaxation:

$$I(\omega) = -\text{Im Sp} \left\{ \sum \rho J_{\alpha}^+ (\omega - \hat{L}_{HF} + i\hat{R} + i\Gamma/2)^{-1} J_{\alpha} \right\}, \quad (9)$$

Here  $\rho$  is the density matrix for the initial state of the Mössbauer ion,  $\omega$  is the frequency of the resonance  $\gamma$ -photon,  $\Gamma$  is the sum of the source and absorber linewidths, the nuclear current density operator  $J_{\alpha}$  describes transitions with polarization  $\alpha$  between the ground and excited nuclear states, the Liouville operator  $\hat{L}_{HF}$  for the static hyperfine interaction determines the positions of the lines in the absence of relaxation, and  $\hat{R}$  is the relaxation operator.

For an axisymmetric crystal field, the spin-lattice relaxation can be described by two parameters  $\gamma_1$  and  $\gamma_2$  (Ref. 6), and the relaxation operator is of the form

$$\hat{R} = a\gamma_1 [(S_z S_+ + S_+ S_z) [(S_- S_z + S_z S_-) \dots]] + b\gamma_2 [S_+^2 [S_-^2 \dots]], \quad (10)$$

where  $a$  and  $b$  are normalization factors,  $S_{\pm} = S_x \pm iS_y$ , and the square brackets denote quantum-mechanical commutators. The parameters  $\gamma_1$  ( $\gamma_2$ ) give the probability that a transition in which the electron spin projection changes by  $|\Delta S_z| = 1$  ( $|\Delta S_z| = 2$ ) will occur from one of the sublevels of the doublet  $|\pm 1/2\rangle$  to a sublevel of the  $|\pm 3/2\rangle$  doublet (Fig. 2b).

The total probability for a transition to a fixed sublevel of the excited doublet is equal to  $\gamma = \gamma_1 + \gamma_2$ , while according to the principle of detailed balance, the probabilities for

the reverse processes are related to  $\gamma_1$  by:

$$\tilde{\gamma}_i = \gamma_i e^{\Delta/T}, \quad \tilde{\gamma} = \tilde{\gamma}_1 + \tilde{\gamma}_2. \quad (11)$$

In an applied magnetic field the wave functions of the electron states transform according to Eqs. (6) and (7), and the corresponding probabilities for transitions between sub-levels of the states  $|1^{(\pm)}\rangle$  and  $|2^{(\pm)}\rangle$  become

$$\Gamma_1 = a_1^2 \gamma_1 + a_2^2 \gamma_2, \quad \Gamma_2 = a_2^2 \gamma_1 + a_1^2 \gamma_2. \quad (12)$$

It is clear from expressions (8) and (12) that due to the strong dependence of the coefficients  $a_1$  and  $a_2$  on the angle  $\theta$ , the relaxation Mössbauer spectrum is very sensitive to the angle between  $\mathbf{H}$  and the symmetry axis  $z$ . For example, if  $\mathbf{H} \perp z$  ( $\theta = 90^\circ$ ) it follows from (8), (12) that  $\Gamma_1 = \Gamma_2 = \gamma/2$ , i.e., a single parameter suffices to describe the relaxation. However, if  $\mathbf{H} \parallel z$  ( $\theta = 0^\circ$ ) we have  $\Gamma_1 = \gamma_1$ ,  $\Gamma_2 = \gamma_2$ , and two parameters are necessary. The two-parameter nature of the spin-lattice relaxation can therefore be observed only when the external magnetic field is nearly parallel to the axis of symmetry.

### 3. EXPERIMENTAL METHOD

Metmyoglobin single crystals measuring  $2 \times 1 \times 0.5$  mm<sup>3</sup> and enriched to 90% with the isotope <sup>57</sup>Fe were grown by the technique used in Ref. 7. The crystals were preserved in a saturated ammonium sulfate buffer solution prior to the measurements to prevent them from denaturing. The measurements were carried out in a helium cryostat equipped with a vacuum fitting, which enabled us to vary the crystal temperature from 4.5 to 300 K. A droplet of buffer solution containing a crystal was mounted on a brass holder, on which two resistance thermometers and two heaters were mounted. For rapid cooling, the holder was immersed in liquid nitrogen and enclosed in a Teflon-sealed cup. The

vacuum fitting was then rapidly evacuated and inserted into a cryostat containing liquid helium.

The external magnetic field was produced by two pairs of permanent ring magnets in the horizontal plane and by one magnet in the vertical plane. By changing the distance between the magnets, we were able to vary the magnitude and orientation of the external magnetic field relative to the crystal within certain limits. Owing to the small crystal size, the magnetic field at the crystals was uniform to within  $\approx 2\%$ .

The Mössbauer spectra were recorded by a standard spectrometer operating at constant gain; the <sup>57</sup>Co(Cr) source was 4 mm in diameter and had an initial activity of  $\approx 250$   $\mu$ C; a proportional counter containing a krypton-neon-methane mixture was used. The instrument linewidth was found to be  $\Gamma_\alpha \approx 0.38$  mm/s by calibration using a standard  $\alpha$ -Fe absorber (the source linewidth was  $\Gamma_s \approx 0.18$  mm/s).

We carried out independent measurements without a crystal in order to find the contribution to the spectrum from iron impurities present in the beryllium windows of the cryostat and vacuum fitting. We found that the impurities gave rise to a slightly unsymmetric doublet with relative intensity  $\approx 0.5\%$ , shift  $\delta \approx 0.4$  mm/s, and splitting  $\varepsilon \approx 0.6$  mm/s; we corrected for this when analyzing the metmyoglobin spectra.

### 4. EXPERIMENTAL RESULTS

Mössbauer spectroscopy was previously employed in Refs. 12, 13 to study metmyoglobin in frozen solution. Investigations of single-crystal specimens revealed<sup>5,14</sup> that the positions of the metmyoglobin spectral lines at helium temperatures depend strongly on the angles  $\theta_\alpha$  between the external field  $\mathbf{H}_e$  and the heme axes  $\mathbf{n}_\alpha$  ( $\alpha = 1, 2$ , Fig. 1). This dependence is steepest for angles  $\theta_\alpha \lesssim 10^\circ$ ; according to Eq. (5), the quantity  $H_{\text{eff}}(\theta)$  decreases by a factor of three when  $\theta$  decreases from 90 to  $0^\circ$ .

The angular dependence  $H_{\text{eff}}(\theta)$  can be used not only to distinguish the contribution of the partial spectra from the inequivalent  $\text{Fe}^{3+}$  sites to the total spectrum of the crystal, but also to obtain an independent method for finding the orientation of the  $\mathbf{n}_\alpha$  axes (Ref. 5). Since the orientation of the crystal axes (except for the  $[b]$  symmetry axis) was not known in advance, we used this method to determine the orientation for our crystal. The result is shown in Fig. 3, which presents spectra recorded in an external "stabilizing" magnetic field. The magnetic inequivalence of the  $\text{Fe}^{3+}$  sites disappears when  $\mathbf{H}_e \perp [b]$ , and their partial spectra coincide (Fig. 3a). A least-squares analysis of this spectrum yielded the following values for the hyperfine splitting parameters: the effective field at the nucleus was  $H_{\text{eff}} = 497 \pm 2$  kG and the quadrupole splitting was  $eQV_{zz}/2 = 1.12 \pm 0.03$  mm/s. These values correspond to the case when  $\mathbf{H}_e$  is nearly perpendicular to  $\mathbf{n}_1$  and  $\mathbf{n}_2$ . By rotating the vector  $\mathbf{H}_e$  and deducing the angles  $\theta_1, \theta_2$  in each case from the corresponding spectrum, it is possible to align  $\mathbf{H}_e$  parallel to one of the heme axes, e.g.,  $\mathbf{n}_1$  (Fig. 3b). This was confirmed both by test spectra, recorded when  $\mathbf{H}_e$  deviated by  $\approx 2^\circ$  in either direction from the axis found by the above procedure, and by computer-simulated spectra calculated using the static Hamiltonian (2). The error in using this technique to determine the orientation of the symmetry axis of paramagnetic

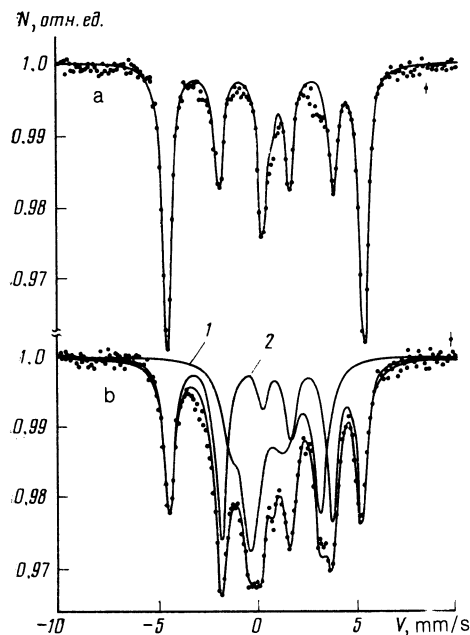


FIG. 3. Mössbauer spectra for metmyoglobin at  $T = 4.2$  K in a "stabilizing" external magnetic field  $H_e = 196$  G: a)  $\theta_1 = \theta_2 \approx 90^\circ$  ( $\mathbf{H}_e \perp [b], \mathbf{n}_{1,2}$ ); b)  $\theta_1 = 0, \theta_2 = 44^\circ$  ( $\mathbf{H}_e \parallel \mathbf{n}_1$ ). 1, 2) partial spectra from  $\text{Fe}^{3+}$  ions at sites 1 and 2, respectively. The solid curves show the results obtained by simulating the spectra 1 and 2 using the static Hamiltonian (2) with a random magnetic field.

complexes in biomolecules containing  $\text{Fe}^{3+}$  in the high-spin state was estimated by direct x-ray analysis to be  $\approx 1^\circ$  (Ref. 5).

Figure 3b further shows that the splitting and linewidth for the partial spectrum from  $\text{Fe}^{3+}$  ions at the sites 2, for which  $\theta_2 \approx 44^\circ$ , are similar to the corresponding values for the spectrum in Fig. 3a, whereas the lines in the partial spectrum for the ions at sites 1 are broadened by the random fields. Setting  $\mathbf{H} = \mathbf{H}_r$  in the Hamiltonian (2) and using the chi-square test to compare the experimental spectrum, recorded without an external field,<sup>5</sup> with the calculated spectra obtained by numerically averaging over  $\mathbf{H}_r$  for different values of the variance  $\overline{H_r}$ , one obtains the estimate  $\overline{H_r} = 13 \pm 3$  G for an isotropic Gaussian distribution.<sup>15</sup> We used the same random magnetic field (RMF) model to calculate both the static and the relaxation spectra in a "stabilizing" field; the average local variation in the orientation of the resultant field  $\mathbf{H} = \mathbf{H}_e + \mathbf{H}_r$ , deduced from these spectra was found to be  $\overline{\theta} \approx 6^\circ$ . The RMF has little effect on the  $\text{Fe}^{3+}$  ions at the sites 2, for which  $\mathbf{H}_e$  deviates substantially from  $\mathbf{n}_2$ ; this is not true, however, for the ions at the sites 1, where they greatly distort the form of the spectrum.

The experimental Mössbauer spectra for a metmyoglobin single crystal in an external magnetic field  $H_e = 196$  G ( $\mathbf{H}_e \parallel \mathbf{n}_1$ ) are shown in Fig. 4 ( $T < \Delta$ ) and Figs. 5 and 6 ( $T \gtrsim \Delta$ ). We see that the lines become broader and shift appreciably upon heating; this is because the spin-lattice relaxation rate increases. The extent of the broadening depends on the partial spectrum to which the lines belong and is determined by the angle between  $\mathbf{H}_e$  and the symmetry axes  $\mathbf{n}_\alpha$  of the complexes. For example, it is clear from Fig. 4 that the broadening for the outermost lines in the spectrum, which lie at  $V \approx -4.5$  mm/s and  $V \approx 5$  mm/s and belong to the partial spectrum from the  $\text{Fe}^{3+}$  complexes at sites 2, is much greater than for the lines in the partial spectrum from the ion complexes at sites 1 (compare, e.g., the line at  $V \approx 3.0$  mm/s).

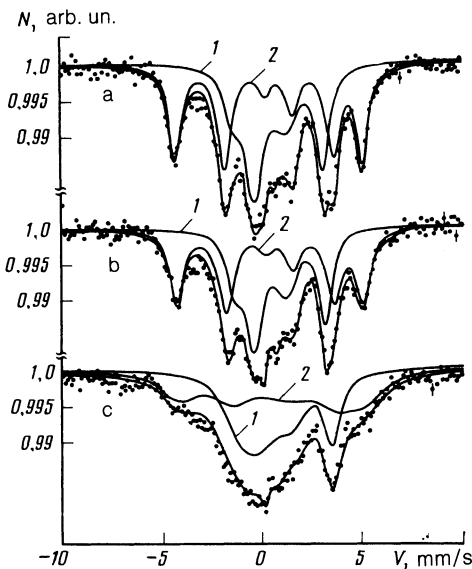


FIG. 4. Mössbauer spectra for metmyoglobin (slow-relaxation case,  $T \lesssim 10$  K) for  $\mathbf{H}_e \parallel \mathbf{n}_1$  ( $\theta_1 = 0$ ,  $\theta_2 = 44^\circ$ ,  $H_e = 196$  G) for  $T = 6.8$  (a), 7.55 (b), and 10.5 K (c). Traces 1 and 2 are the same as in Fig. 3. The solid curves give simulated results in which perturbation theory (13), (14) is used to treat the effects of the relaxation on the spectrum.

We found the relaxation parameters  $\gamma_1$  and  $\gamma_2$  and their temperature dependence by using the theory discussed in Sec. 2 to numerically simulate the Mössbauer spectra for metmyoglobin. The spectra recorded at  $T = 4.5$  K were used as a reference; at this temperature the doublet  $|\pm 3/2\rangle$  is virtually unpopulated, and the relaxation can be neglected (Fig. 3). Under these conditions the hyperfine spectrum is static, and the width and position of the lines depend only on the angle  $\theta$ .

Perturbation theory can be used to treat the deformation of the static Mössbauer spectrum when the relaxation is slow, i.e., for  $\gamma \ll \omega_{HF}$ , where  $\omega_{HF}$  is the characteristic interval between the hyperfine sublevels. This condition holds for metmyoglobin if  $T \lesssim 10$  K (Fig. 4), for which the doublet  $|\pm 3/2\rangle$  is still essentially unpopulated. Neglecting terms  $\propto \exp(-\Delta T)$ , we obtain

$$I(\omega) = -\text{Im} \sum_l D_l [\omega - \omega_l^{(1)} + \delta\omega_l + i(\gamma + \Gamma/2)]^{-1}, \quad (13)$$

for the spectral function in the slow-relaxation case. Here  $D_l$  is the intensity of the  $l$ th line in the static spectrum,

$$\delta\omega_l = \sum_k R_{lk} R_{kl} [\omega_l^{(1)} - \omega_k^{(2)} + i\tilde{\gamma}]^{-1}, \quad (14)$$

the  $\omega_l^{(i)}$  are the frequencies for the transitions between the sublevels of the static hyperfine structure for the  $i$ th doublet, and the  $R_{lk}$  are the matrix elements of the relaxation operator in a basis diagonalizing the matrix  $\hat{L}_{HF}$ .

Since no small parameter is available for the case of intermediate relaxation ( $T \gtrsim \Delta$  and  $\gamma \sim \omega_{HF}$ ), the Mössbauer spectrum can be found only by an exact calculation using Eq. (9). This amounts to inverting the matrix  $(\omega - \hat{L}_{HF} + i\hat{R} + i\Gamma/2)$ , which is of rank  $N = 4(2I_e + 1)(2I_g + 1) = 32$  ( $I_e$  and  $I_g$  are the nuclear spins in the excited and ground states). It can be shown that the change of basis

$$|p_{1,2}\rangle = 2^{-1/2} \{ |i^{(+)}\rangle, m_g \langle m_g, i^{(+)} | \pm |i^{(-)}\rangle, -m_g \langle -m_g, i^{(-)} | \} \quad (15)$$

decomposes the above matrix into blocks of rank 16. In Eq. (15),  $p_{1,2} = 1, 2, \dots, 16$  labels the basis functions, the  $|i^{\pm}\rangle$  are the wave functions for the Kramers doublet, and  $m_g$  and  $m_e$  are the projections of the nuclear spin on the symmetry axis in the ground and excited states, respectively. In this case the relaxation spectra were simulated numerically by diagonalizing the two  $16 \times 16$  matrices and summing over their eigenvectors (see, e.g., Ref. 16).

We used perturbation theory to allow for the small population of the doublet  $|\pm 5/2\rangle$ , which begins to have an effect when  $T > \Delta$ ; this gave small corrections to the line widths and positions.

The solid traces in Fig. 5 show the calculated resultant spectra, together with the partial spectra from each type of complex; the results are seen to agree closely with experiment. The values of  $\gamma_1$  and  $\gamma_2$  were found for each recorded spectrum, and their temperature dependence deduced in this way is shown in Fig. 7. It agrees closely with the theoretically predicted dependence<sup>9</sup> for single-phonon processes:

$$\gamma_i = C_i [e^{\Delta/T} - 1]^{-1} \quad (16)$$

with constants  $C_1 = 5.4 \pm 0.2$  mm/s and  $C_2 = 0.40 \pm 0.05$  mm/s.

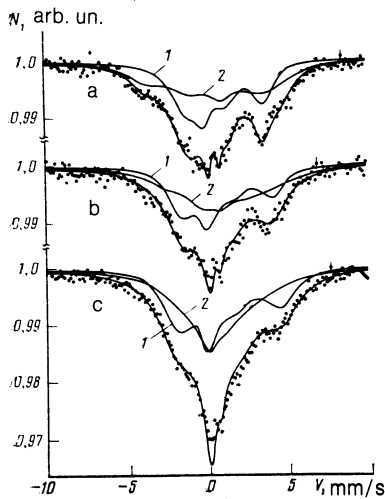


FIG. 5. Mössbauer spectra for metmyoglobin in the intermediate relaxation case ( $T \gtrsim \Delta$ ) for  $H_e \parallel n_1$ , at  $T = 14.3$  (a), 30 (b), and 40 K (c). The solid traces show numerical calculations using the complete equation (9). Curves 1, 2 are as in Figs. 3 and 4.

Analysis of a large body of experimental and theoretical work (see, e.g., Refs. 3 and 17) on the  $Fe^{3+}$  ion in the high-spin state indicates that there is a wide range of temperatures for which spin-lattice relaxation occurs via direct one- and two-phonon processes. The contribution from these processes is sensitive to the ratio  $\Theta_D/\Delta$ , where  $\Theta_D$  is the Debye temperature and  $\Delta$  is the characteristic spacing between the electron levels. For  $T \gtrsim \Theta_D$  we have

$$P_1/P_2 \sim (\Delta/\Theta_D)^3 \Theta_D/T, \quad (17)$$

where  $P_1$  and  $P_2$  are the probabilities for one- and two-phonon transitions, respectively. For most crystals (particularly inorganic ones) that contain the  $Fe^{3+}$  ion,  $\Delta/\Theta_D$  is  $\sim 10^{-2}$ – $10^{-4}$ , so that two-phonon relaxation is much faster than one-phonon relaxation.

For metmyoglobin, however, the large splitting  $\Delta$  and small  $\Theta_D$  combine to make one-phonon transitions dominant for temperatures 4–60 K. For  $T$  above 60 K, (17) shows that two-phonon processes eventually dominate.

The smallness of the ratio  $\gamma_2/\gamma_1 \approx 0.07$  is striking and at first glance would appear to indicate that only the single parameter  $\gamma = \gamma_1$  is needed to describe the relaxation pro-

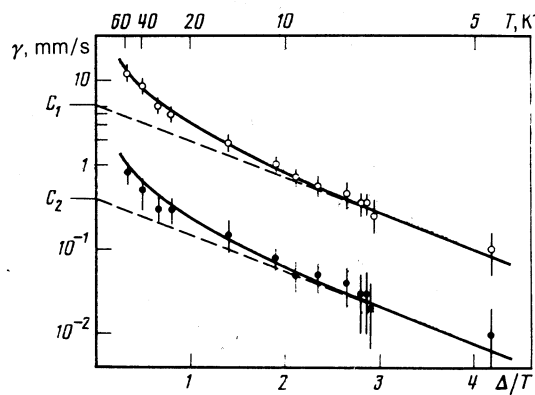


FIG. 7. Temperature dependence of the relaxation parameters for  $Fe^{3+}$  in metmyoglobin, shown on a logarithmic scale (the light and dark circles give  $\gamma_1$  and  $\gamma_2$ , respectively). The solid curves were calculated by Eq. (16) with constants  $C_1 = 5.4$  mm/s and  $C_2 = 0.40$  mm/s; 1 mm/s corresponds to a relaxation frequency of 72.9 MHz.

cess. However, our simulations show that the shape of the spectrum is very sensitive to the parameter  $\gamma_2$  (see Fig. 6) and in fact can be used to deduce  $\gamma_2$  quite accurately. The marked difference in the values of  $\gamma_1$  and  $\gamma_2$  can be shown to imply that the thermal vibrations of the ligands in the  $Fe^{3+}$  paramagnetic complex must be strongly anisotropic.

Because the nearest-neighbor structure for the Mössbauer ion in metmyoglobin is nearly octahedral, to a first approximation the vibrations of the complex can be described in terms of six normal coordinates  $Q_f$  ( $f = 1, \dots, 6$ ) (Ref. 18). For single-phonon processes the crystal field potential  $V$  can be expanded as a power series in  $Q_f$ ; keeping only the linear terms, one obtains

$$V = V_0 + \sum_f \left( \frac{\partial V}{\partial Q_f} \right)_0 Q_f + \dots \quad (18)$$

Expressing  $V_0$  and  $(\partial V/\partial Q_f)_0$  in terms of the equivalent spin operators  $S_i$ , we obtain the so-called dynamic spin Hamiltonian for the crystal field, for which an explicit expression has been given by Leushin.<sup>19</sup> The term  $V_0$  then describes the static part of the Hamiltonian in (1), while the

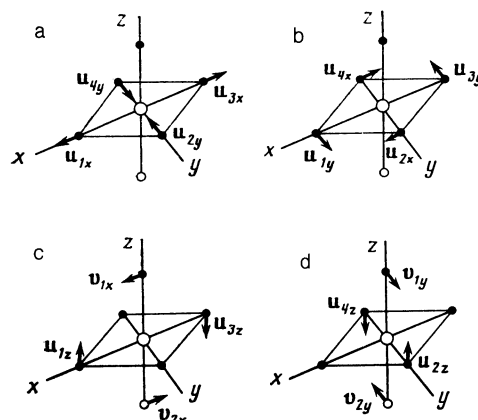


FIG. 8. Sketch showing the thermal vibrations of the nearest-neighbor atoms surrounding an  $Fe^{3+}$  ion in a metmyoglobin molecule for the following normal modes of the octahedral complex: a)  $Q_2$ ; b)  $Q_4$ ; c)  $Q_5$ ; d)  $Q_6$ . The arrows show the displacement vectors of the nitrogen atom in the plane of the heme ( $u_i$ ) and of the nitrogen atom and water molecule on the heme axis ( $v_j$ ). The  $Fe^{3+}$  ion lies at the center, while the light and dark circles represent  $H_2O$  and  $N$ , respectively.

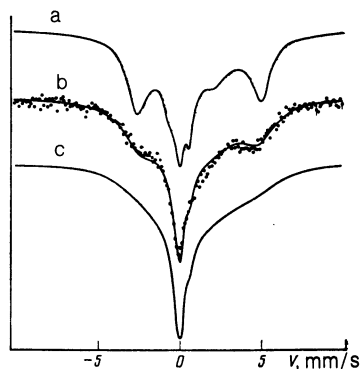


FIG. 6. Mössbauer spectrum for metmyoglobin at  $T = 57$  K for  $H_e \parallel n_1$ . The traces show that the calculated relaxation spectra depend on the small relaxation parameter  $\gamma_2$  ( $\gamma_1 = 12$  mm/s): a)  $\gamma_2 = 0$ ; b)  $\gamma_2 = 0.6$  mm/s; c)  $\gamma_2 = 1.5$  mm/s.

other term describes the relaxation. One can show that the parameters  $\gamma_i$  are related to the normal vibrations  $Q_i$  as follows:

$$\gamma_1 \propto (Q_5^2 + Q_6^2), \quad \gamma_2 \propto (e^2 Q_2^2 + Q_4^2), \quad (19)$$

where the constant  $\varepsilon$  is expressible in terms of the electron energy levels of the paramagnetic ion. The relation  $\gamma_1 \gg \gamma_2$  and Eqs. (19) imply that in the specific case of myoglobin, the vibrations of the nitrogen atom in the heme plane, described by the modes  $Q_2$  and  $Q_4$ , are much weaker than the  $Q_5$  and  $Q_6$  vibrations in the plane passing through the heme axis (Fig. 8).

## 5. CONCLUSIONS

In terms of its influence on the Mössbauer spectra, the multiparametric nature of the spin-lattice relaxation process should show up most clearly when the effective hyperfine fields  $H_{\text{eff}}^{(j)}$  for the electron sublevels involved in the relaxation transitions are almost parallel. If the orientations of the  $H_{\text{eff}}^{(j)}$  differ markedly, the relaxation transitions lead to strong mixing of the hyperfine sublevels and the relaxation is effectively averaged out over the sublevels. For the case of  $\text{Fe}^{3+}$  in myoglobin, the first situation occurs when the external field is parallel to the heme axis, while the second situation occurs when it deviates markedly from the heme axis.

An alternative multi-parametric description of spin-lattice relaxation was considered in Ref. 20, where Mössbauer spectra for  $\text{Fe}^{3+}$  in  $\text{NH}_4\text{Al}(\text{SO}_4)_2 \cdot 12\text{H}_2\text{O}$  were studied for strong magnetic fields satisfying  $\mathcal{H}_Z \gg \mathcal{H}_{CF}$ . However, the polycrystalline specimen used there made it impossible to observe the multi-parametric relaxation in the spectra, because the parameters  $\gamma_1$  and  $\gamma_2$  depend on the direction of the external field relative to the crystallographic axes. This apparently also explains why, in the overwhelming majority of experiments on spin-lattice relaxation using Mössbauer spectroscopy, it has been possible to describe the tempera-

ture dependence of the spin-lattice relaxation in a satisfactory way using only a single parameter.

We are grateful to V. Ya. Goncharov for great assistance in designing the experiment.

<sup>1)</sup>Institute of Physical Chemistry, Münster, West Germany.

- <sup>1</sup>M. J. Clouser and M. Blume, *Phys. Rev. B* **3**, 583 (1971).
- <sup>2</sup>A. M. Afanas'ev, *Proc. ICAME*, Vol. 1, Gordon and Breach Sci. Publ., New York (1985), p. 23.
- <sup>3</sup>I. P. Suzdalev, A. M. Afanas'ev, A. S. Plachinda, *et al.*, *Zh. Eksp. Teor. Fiz.* **55**, 1752 (1968) [*Sov. Phys. JETP* **28**, 923 (1968)].
- <sup>4</sup>A. M. Afanas'ev and Yu. M. Kagan, *Pis'ma Zh. Eksp. Teor. Fiz.* **8**, 620 (1968) [*JETP Lett.* **8**, 382 (1968)].
- <sup>5</sup>S. S. Yakimov, V. M. Cherepanov, M. A. Chuev, *et al.*, *Hyperfine Interactions*, Vol. 14, p. 1, *Proc ICAME* (1983). N.Y.: Gordon and Breach Sci. Publ., Vol. 4, p. 1519 (1985).
- <sup>6</sup>A. M. Afanas'ev, E. Yu. Tsybal, and O. A. Yakovleva, *IAE Preprint No. 4272/9*, Moscow (1986).
- <sup>7</sup>J. C. Kendrew and R. G. Parrish, *Proc. R. Soc. A* **238**, 305 (1957).
- <sup>8</sup>A. L. Gray and H. A. Buckmaster, *Canad. J. Biochem.* **51**, 1142 (1973).
- <sup>9</sup>A. Abragam and B. Bleaney, *Electron Paramagnetic Resonance of Transition Ions*, Clarendon Press, Oxford (1970).
- <sup>10</sup>A. M. Afanas'ev, V. D. Gorobchenko, I. Dezhi, *et al.*, *Zh. Eksp. Teor. Fiz.* **62**, 673 (1972) [*Sov. Phys. JETP* **35**, (1972)].
- <sup>11</sup>A. M. Afanas'ev and V. D. Gorobchenko, *Zh. Eksp. Teor. Fiz.* **66**, 1406 (1974) [*Sov. Phys. JETP* **39**, 690 (1974)].
- <sup>12</sup>G. Lang, T. Asakura, and T. Yonetani, *Phys. Rev. Lett.* **24**, 981 (1970).
- <sup>13</sup>U. F. Thomanek, F. Parak, S. Formanek, and G. M. Kalvius, *Biophys. Struct. Mech.* **3**, 207 (1977).
- <sup>14</sup>T. Harami, *J. Chem. Phys.* **71**, 1309 (1979).
- <sup>15</sup>J. Hess and A. Levy, *Phys. Rev. B* **22**, 5068 (1980).
- <sup>16</sup>M. J. Clouser, *Phys. Rev. B* **3**, 3748 (1971).
- <sup>17</sup>K. K. P. Srivastava and S. N. Mishra, *Phys. Status Solidi (b)* **100**, 65 (1980).
- <sup>18</sup>S. A. Al'tshuler and B. M. Kozyrev, *Élektronnyĭ Paramagnitnyĭ Rezonans Soedineniĭ Elementov Promezhutochnykh Grupp (Electron Paramagnetic Resonance in Intermediate-Group Compounds)*, Nauka, Moscow (1972), Chap. 5.
- <sup>19</sup>A. M. Leushin, *Fiz. Tverd. Tela* **5**, 605 (1963) [*Sov. Phys. Solid State* **5**, 440 (1963)].
- <sup>20</sup>S. C. Bhargava, J. E. Knudsen, and S. Morup, *J. Phys. C* **12**, 2879 (1979).

Translated by A. Mason